Nonequilibrium dynamics of quasiparticles in superconductors

S. Sridhar* and J. E. Mercereau
Low Temperature Physics 63-37, California Institute of Technology, Pasadena, California 91125
(Received 24 January 1986)

Small changes δR_s in the 10-GHz surface resistance R_s of thin superconducting films of Sn and In, caused by an induced static current J_0 have been measured. δR_s was quadratic in J_0 and both increases ($\delta R_s > 0$) and decreases ($\delta R_s < 0$) of absorption were observed. The increase is associated mainly with thermodynamic depression of the gap parameter due to the static current. On the other hand, the decrease of absorption, which implies an enhancement of superconductivity, is incompatible with thermodynamic analysis. A nonequilibrium analysis is presented, according to which the combined static and high-frequency currents cause a nonthermal, time-dependent oscillation of the quasiparticle distribution, and which is out of phase with the driving high-frequency field. The counter oscillation leads to an enhancement of high-frequency supercurrent and decrease of dissipative normal current, and hence results in a decrease of absorption. The analysis describes the experimental results for very thin films of Sn both qualitatively and quantitatively, and with no adjustable parameters. These results lead to the conclusion that at high frequencies, the superconductor responds to time-dependent perturbations in an inherently nonadiabatic, nonequilibrium manner even for vanishingly small high-frequency fields. The implications for several unexplained experiments on the magnetic field dependence of R_s are discussed.

INTRODUCTION

Unexplained effects in the dynamic high-frequency response of superconductors in the presence of static perturbations such as magnetic fields or applied currents have been observed since the first experiments of Pippard.[1] A complete understanding of such phenomena has remained elusive,[2] despite a variety of experiments carried out over a wide range of frequency and materials parameters. In this paper, we report on recent measurements[3,4] and analyses of the microwave response of thin superconducting films in the presence of an induced static current. Our proposed interpretation of these novel results, which is successful both qualitatively and quantitatively, leads to the important conclusion that nonequilibrium effects play a vital role in the description of dynamical effects in superconductors at high frequencies.

The measurements are of changes δR_s of the microwave (10 GHz) surface resistance R_s of thin superconducting films of Sn and In, caused by a static supercurrent of density J_0 induced in the films by a magnetic field B_0 applied on one side of the film. We have observed both *increases* ($\delta R_s > 0$) occurring at high temperatures near the transition temperature T_c and, *more surprisingly, decreases* ($\delta R_s < 0$) at low temperatures. δR_s was observed to be quadratic in J_0 (or B_0) over the entire temperature range studied ($0.3 < T/T_c < 0.98$) except in the narrow range of temperature where δR_s changed sign. We describe the results in terms of a reduced temperature t and thickness d dependent parameter $k(t,d)$ and maximum surface field B_0:

$$\frac{\delta R_s(B_0)}{R_s(0)} \equiv \frac{R_s(B_0)-R_s(0)}{R_s(0)} = k(t,d)B_0^2 \ . \qquad (1)$$

For very thin films, the parameter $k(t,d)$ was positive ($\delta R_s > 0$) near T_c and negative ($\delta R_s < 0$) at low temperatures.

The observed increase of R_s can be understood within a thermodynamic framework: the static current increases the free energy of the film, "pushing" it toward the normal state, and hence decreases the gap parameter resulting in increased absorption. Near T_c, where the increased absorption is observed, the measurements agree quantitatively with a Ginzburg-Landau description of the order-parameter reduction.

On the other hand, the observed decrease of R_s, which implies an enhancement of superconductivity, cannot be understood in terms of such a macroscopic thermodynamic description. Instead, we find that a more complete description in the context of recent theories of nonequilibrium superconductivity is required. We have employed the formalism[5,6] of a microscopic theory of the dynamic nonequilibrium quasiparticle response in the presence of a static current, which is applicable in the local electrodynamic limit and at high frequencies $\omega\tau_{in} \gg 1$, where τ_{in} is the inelastic quasiparticle scattering time.[7] Numerical calculations agree quantitatively with the experimental results for very thin films with no adjustable parameters. This is the first time that the nonequilibrium quasiparticle response has been analyzed and applied to this type of problem, and also that agreement between theory and experiment has been found for this class of experiments.

In the framework of the analysis, the superposed static and high-frequency currents lead to dynamic pair-breaking effects, due to which the density of quasiparticle states oscillates in phase with the high-frequency field. If the driving frequency is smaller than the quasiparticle inelastic relaxation rate ($\omega < 1/\tau_{in}$), then the total quasiparticle number adiabatically follows the instantaneous driv-

ing field and oscillates with it. This mechanism leads to an increase of R_s in the low-frequency regime and is in addition to the increase caused by the depression of the gap parameter. In this adiabatic regime, the thermal equilibrium Fermi distribution function applies for the quasiparticles, while the instantaneous quasiparticle number is determined by the instantaneous density of states.

On the other hand, in the high-frequency limit ($\omega > 1/\tau_{in}$), the quasiparticle number cannot adiabatically follow the field. Instead, the distribution function develops a high-frequency component out of phase with the density of states (and hence with the driving field) in order to maintain an unchanging total quasiparticle number. *This out-of-phase, nonthermal oscillation of the distribution function leads to an enhancement of the high-frequency supercurrent and a decrease of dissipative normal current resulting in a decrease of* R_s. This effect dominates at low temperatures over the increase of R_s due to gap parameter reduction. Numerical calculations are in quantitative agreement with experimental results for very thin films of Sn over the entire temperature range studied.

For thick Sn films with $d \gtrsim 800$ Å, δR_s was again quadratic in B_0 (or J_0) but was positive [$k(t,d) > 0$] at all temperatures. We attribute this to nonlocal electrodynamic effects which are not included in the present theory.

In the context of nonequilibrium superconductivity,[8] microwaves play a unique role as both a perturbation and probe of the nonequilibrium superconducting state. The microwave-induced distribution function discussed in this work corresponds to the L (longitudinal) mode of Schmid and Schön,[9] whereas thermoelectric and branch imbalance phenomena correspond to the T (transverse) mode. The present experiments are related to the gap enhancement and order-parameter relaxation experiments.[10] A unique aspect of the present results is the nonequilibrium response of the superconductor even for a vanishingly small microwave field, so long as the microwave frequency $\omega > 1/\tau_{in}$. This is due to the presence of the static current. In contrast, for the cases of gap enhancement and nonlinear impedance, the nonequilibrium state is determined by the strength of the microwave magnetic field.

This paper is organized as follows: Section I discusses the experimental procedure and Sec. II the experimental results. Section III presents a summary of the nonequilibrium "dirty"-limit theory and discusses the relevant physical processes. Section IV is a comparison of experiment and theory and also discusses the relationship to earlier bulk experiments. This is followed (Sec. V) by a comparison of the present results and conclusions with previous work. Finally, in the Appendix, detailed expressions for the theory of Sec. III are provided.

I. EXPERIMENTAL CONFIGURATION

The experiment was designed to measure both the absolute surface resistance R_s and changes δR_s of R_s. This was accomplished by utilizing a thin-film test sample (evaporated on a sapphire disc) as one wall of a fully superconducting microwave cavity (Fig. 1), resonant at 10.12 GHz in the TE_{011} mode. The remainder of the resonator surface was Pb plated on oxygen-free high-conductivity (OFHC) Cu. The resonator Q was dominated by the film absorption since the Pb surface, having a higher transition temperature T_c, contributed only 1% to the total absorption. (For further details see Ref. 4.)

Measurement of the resonator Q yielded the absolute value of the surface resistance: $R_s = \Gamma/Q$. The value of $\Gamma = 2970\ \Omega/\text{sq}$ was determined by the mode geometry (TE_{011}) and the inhomogeneous resonator surface, i.e., the greater contribution of the thin film relative to the negligible contribution of the Pb surface. Depending on temperature, the resonator Q varied from 10^4 to 10^9. The coupling system was specifically designed to weakly or critically couple over this entire range of Q's.

Static current (J_0) was induced in the film by applying a static magnetic field B_0, produced by a coil, to one side of the film (Fig. 1). The superconducting film shields out the magnetic field on the resonator side, due to which currents (J_0) are induced in the film. These currents have the same cylindrical symmetry and approximate radial spatial configuration as the microwave currents (J_ω). The distribution of J_0 and J_ω through the film depends on its thickness. For films with thickness $d < \lambda$ (the actual or mean-free-path-corrected penetration depth), both currents are nearly uniform and overlap completely through the film. When $d \gtrsim \lambda$, the currents decay into the film. In the present experiment, where the B_0 and B_ω fields are applied on opposite sides of the film, the gradient of the currents into the films is opposite for the two fields, and the overlap is reduced for thick films. If the film response were purely local, this reduced overlap would lead only to a reduced magnitude of δR_s as the thickness was increased. However, as we discuss later, the

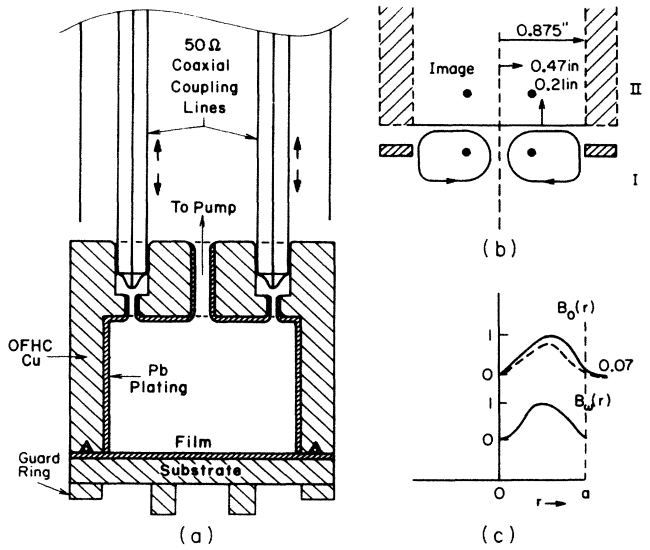

FIG. 1. Experimental configuration and profile of applied fields used to measure $k(t,d)$. (a) Microwave resonator with film and coil which produces magnetic field. (b) Coil and its image and resultant magnetic field lines. (c) Radial profile of static B_0 and high-frequency B_ω fields. Dashed line is a sketch of field profile in the presence of the superconducting guard ring.

thicker films have a nonlocal response, leading to qualitative differences between thin and thick films.

The induced static current changes the surface resistance and hence the resonator Q. These changes were measured using the circuit of Fig. 2. The electronics consisted of two basic parts—a microwave and a data-acquisition subsystem. The former was used to run the resonator in a self-excited phase-locked loop in order to compensate for random drifts in source frequency. The cavity output was heterodyned to an i.f. of 60 MHz and detected with a square-law detector. Thus a steady voltage V_0 was obtained proportional to the resonator Q, since the coupling ports are weakly coupled.

The static current was induced in the form of a triangular wave at 40 Hz. The resulting changes δV (due to changes δQ and thus of δR_s) were detected using the data-acquisition subsystem. The latter, which was fully computerized, carried out an analog-to-digital conversion of 400 points for every 40-Hz period. The results were averaged many times in order to increase the signal-to-noise ratio. By this procedure the normalized changes $\delta R_s/R_s=-\delta Q/Q=-\frac{1}{2}\delta V/V_0$ could be measured to better than 10^{-5}. Since R_s can be as small as 10^{-5} Ω/sq, we *have been able to measure changes* $\delta R_s \gtrsim 10^{-10}$ Ω/sq.

Typical results are displayed in Fig. 3 for the changes $[-\delta V \propto \delta R_s$, Figs. 3(a) and 3(b)] in detector voltage at two representative temperatures (a) $t=0.92$, (b) $t=0.70$. The plots are of the voltage changes δV in response to the instantaneous field (also shown as a triangular waveform). In Fig. 3(a), δR_s *increases* with B_0, while in Fig. 3(b), δR_s *decreases* with B_0.

The resulting digitized data were analyzed on a VAX 11/45 using a polynomial-fitting program. The polynomial dependence of $\delta R_s/R_s$ on the static applied field B_0 was determined and found to be quadratic (except in narrow regions of temperature). The coefficient of the quadratic was calculated from the relation

$$k(t)=2.1\left[\frac{1}{2}\frac{d^2}{dB_0^2}\left[\frac{\delta V}{V_0}\right]\right],$$

where the prefactor 2.1 enters because of the different radial configurations of the static field (B_0) and the high-frequency field B_ω. The above equation represents the result if a *uniform* field B_0 equal to the maximum of the radial distribution were applied to the film.

We now discuss samples and their characterization. All samples studied were films of thickness between 200 and 2000 Å of Sn or In, flash evaporated onto a 2.25-in.-diam $\times 0.125$-in.-thick sapphire disc. The substrate was cooled to 77 K and the evaporation carried out at a pressure of 5×10^{-7} Torr. High-quality mirrorlike films were obtained which were free of pinholes. Examination with a scanning electron microscope (SEM) revealed that the grain size was less than 500 Å.

Measurements of the resonator Q (in the absence of static current) yielded absolute values for the normal state (R_n) and the superconducting (R_s) surface resistance using the relation $R=\Gamma/Q$. R_n yielded the electronic mean free path (MFP l) for the films, via the free-electron relation,[11] $\rho_n l=0.061$ ($\mu\Omega$ cm)μm, and the thin-film result, $\rho_n=R_n/d$. These values are listed in Table I. As the thickness decreased the MFP l is observed to be limited by boundary scattering.

From the measured MFP l, the corrected penetration depth and the coherence lengths in the dirty limit are

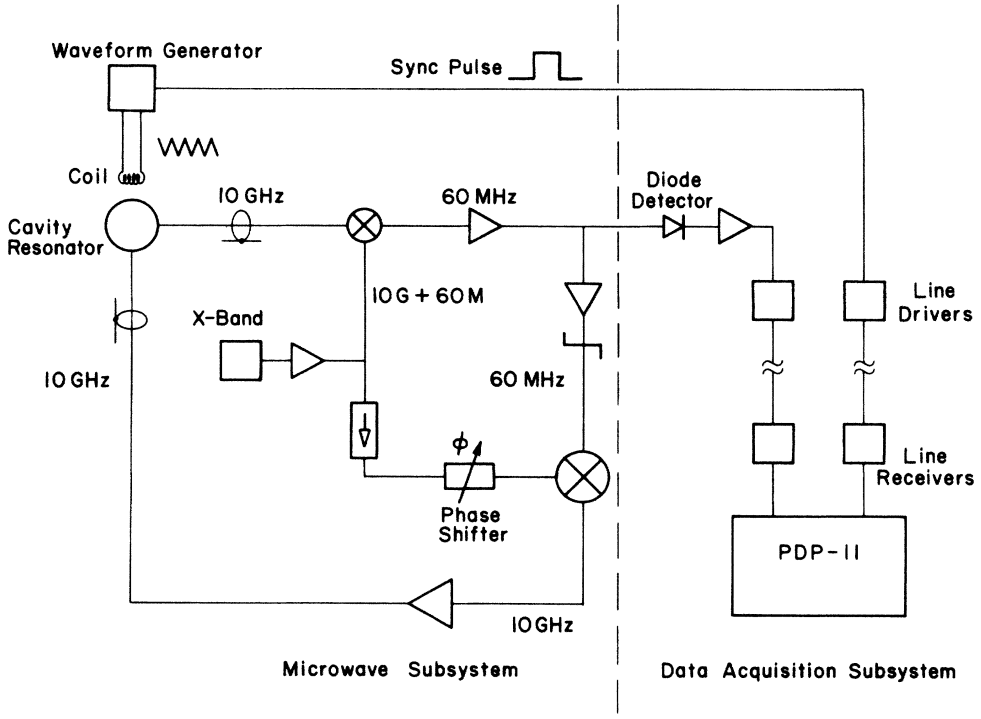

FIG. 2. Microwave and data acquisition systems used to measure $-\delta V \propto \delta R_s$.

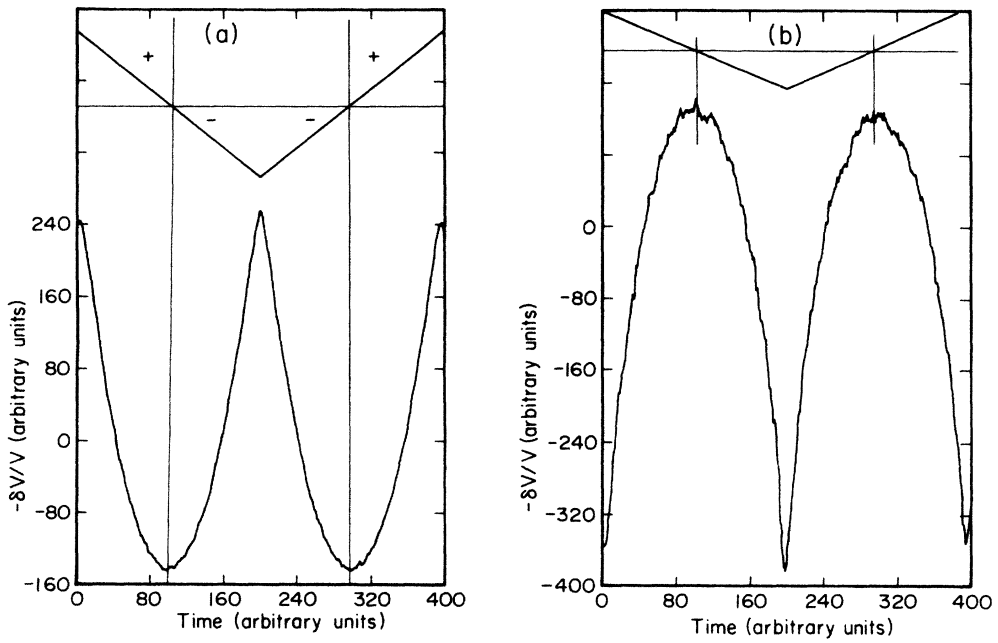

FIG. 3. Typical raw data for $-\delta V \propto \delta R_s$ for film $d = 500$ Å displaying the quadratic behavior on applied static field, whose triangular waveform is displayed on top of each figure. (a) $t = 0.92$, typical of data for $t > 0.88$. Note that $\delta R_s > 0$. (b) $t = 0.70$, typical of data for $t < 0.88$. Note that $\delta R_s < 0$.

evaluated using the expressions[13] $\lambda = \lambda_p(0)(1 + 1.33\xi_0/l)^{1/2}$ and $\xi = 0.85(\xi_0 l)^{1/2}$. The values $\lambda_p(0) = 501$ Å and $\xi_0 = 2300$ Å were used for the pure-limit London penetration depth and coherence length, respectively, for Sn. The resultant values for ξ and λ are listed in Table I.

The measured values of $R_s(t,d)$ were found to agree excellently with the BCS theory corrected for thin-film electrodynamics, using only the measured parameters listed in Table I. The experimental data are plotted as functions of reduced temperature in Fig. 4. The solid lines represent numerical calculations[4] based on the detailed BCS theory; the agreement is clearly excellent. Comparison with simpler expressions applicable to the case of local electrodynamics revealed that for $d < 800$ Å the electrodynamics was local, consistent with shorter mean free paths, while for greater thickness a nonlocal description was necessary.

The above results are important towards the characterization of the films, since they clearly demonstrate that the BCS mechanism is the dominant cause of the microwave response in these films. Consequently, changes in R_s due to static current can be expected to be understood on the basis of extensions of the BCS theory to include nonlinear effects.

TABLE I. Material characteristics of Sn films studied.

d (Å)	l (Å)[a]	λ (Å)[b]	ξ (Å)[c]
260	240	1460	640
500	300	1326	714
800	450	1122	875
1000	510	1069	931
2000	680	960	1069

[a]From the normal-state resistivity ρ_n: $l(\text{Å}) = 610/\rho_n$, ρ_n in $\mu\Omega$ cm.
[b]$\lambda = \lambda_p(0)\,(1 + \xi_0/1.33l)^{1/2}$, $\lambda_p(0) = 510$ Å, $\xi_0 = 2300$ Å.
[c]$\xi = 0.85(\xi_0 l)^{1/2}$.

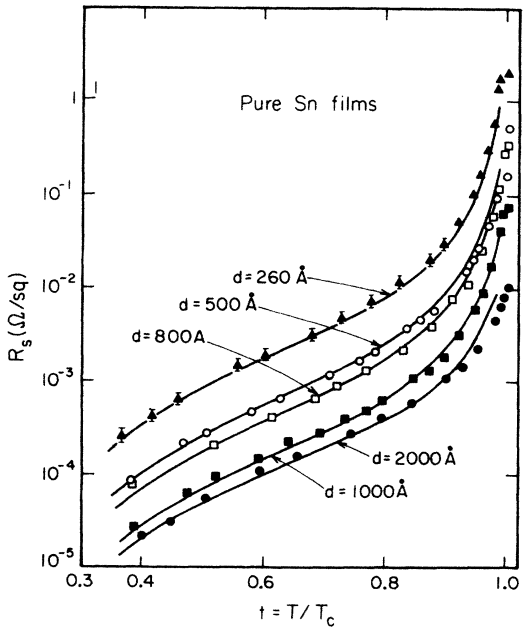

FIG. 4. Experimental results for the surface resistance R_s (at zero-induced static current) for the films studied in this work. The solid lines represent calculations based on the BCS theory (Ref. 4) using the parameters of Table I.

II. EXPERIMENTAL RESULTS

Over most of the temperature range studied [$(0.35–0.98)T_c$] the results for the dependence of R_s on the static field B_0 for the Sn and In films examined could be represented as (see Fig. 3)

$$R_s(B_0,t,d)=R_s(0,t,d)[1+k(t,d)B_0^{2\pm0.05}] . \quad (2)$$

This leads to the normalized change in R_s as in Eq. (1).

The experimental procedure described in the last section was used to measure $k(t,d)$. The experimental uncertainties in $k(t,d)$ arise due to two causes. The first, which is a relative error, is due to random uncertainties and is 10%. The second is a systematic uncertainty in the absolute value of $k(t,d)$ due to the uncertainty of the spatial distribution of the applied static field. It should be emphasized that this error, estimated to be 30%, is temperature independent and solely due to geometric effects.

Experimental measurements for the absolute value of $k(t,d)$ as a function of reduced temperature t are displayed in Fig. 5 for two Sn films with thickness $d=260$ and 500 Å, in Fig. 6 for Sn films with $d \geq 800$ Å, and in Fig. 7 for an In film with $d=500$ Å. We observe the following.

(i) At temperatures between approximately $0.9T_c$ to $0.98T_c$ for the Sn films, $k(t,d)>0$. Thus, $\delta R_s>0$, i.e., the absorption increases.

(ii) At temperature below $\sim 0.88T_c$ (and down to the lowest temperature of $0.35T_c$), $k(t,d)<0$. Here, $\delta R_s<0$,

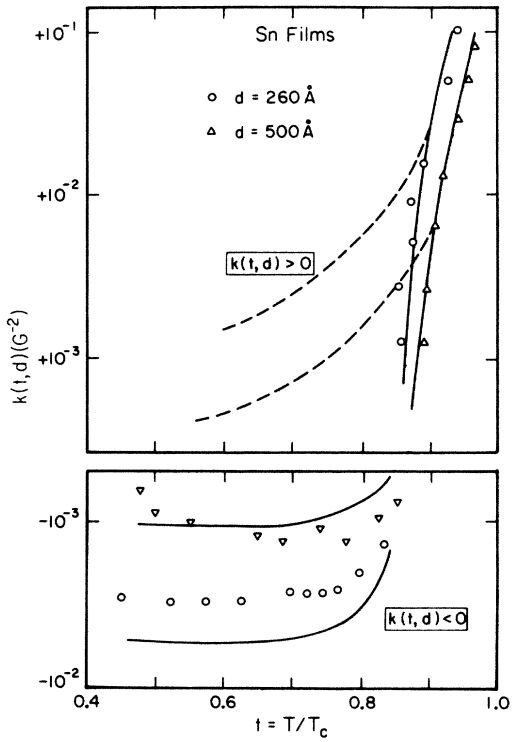

FIG. 5. Experimental results for $k(t,d)$ versus reduced temperature t for very thin films of Sn. Note the logarithmic axis and the sign change. The solid line represents calculations based on the nonequilibrium theory Eq. (12) and the dashed line the Ginzburg-Landau theory Eq. (13).

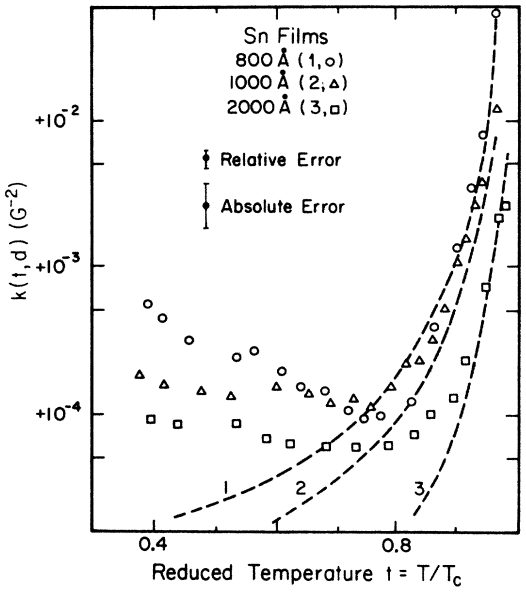

FIG. 6. Experimental results for $k(t,d)$ for thicker films of Sn. The dashed line represents calculations based on the Ginzburg-Landau theory Eq. (13).

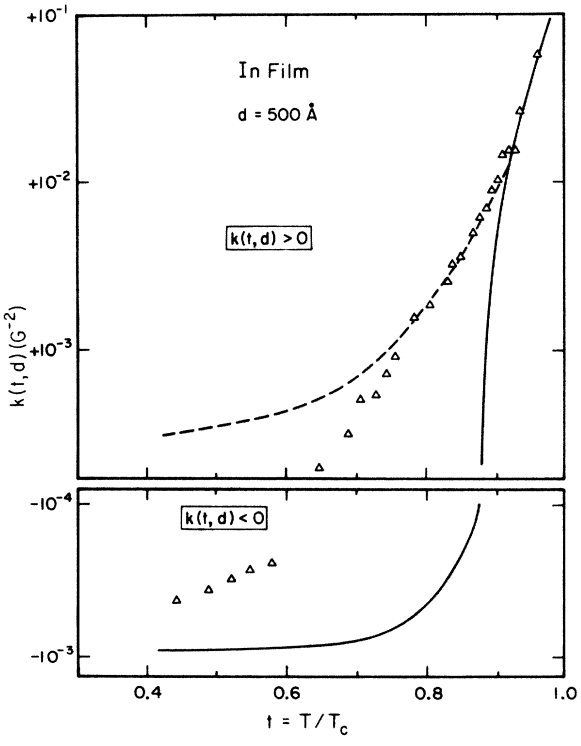

FIG. 7. Experimental results for $k(t,d)$ for an In film $d=500$ Å. Note again the logarithmic axis and the sign change. The solid line represents calculations based on the nonequilibrium theory Eq. (12) and the dashed line the Ginzburg-Landau theory Eq. (13).

the absorption decreases, and we get a novel enhancement of superconductivity.

(iii) The results for the In film are qualitatively similar except that the change in sign from $k>0$ to $k<0$ occurs at a lower temperature between $0.58T_c$ and $0.65T_c$.

Further relevant comments are the following.

(i) The measured changes δR_s in R_s were independent of the microwave field strength B_ω at the film surface and hence were also independent of the absorbed microwave power. This *experimental result,* in addition to demonstrating that an analysis based on Eq. (5) is applicable, also rules out thermal heating (i.e., a real increase in temperature due to absorption) as a factor in these experiments.

(ii) In the narrow regions of temperature ($t\approx 0.88$–0.90 for Sn and $0.58<t<0.65$ for In), where the quadratic coefficient $k\approx 0$, the dependence of δR_s on B_0 was observed to be nonmonotonic. For In at $t=0.60$, clear oscillations were observed with a period of ≈ 0.30 G. While the origin of these effects is not exactly known, we expect that it might be due to motion of trapped flux.

(iii) When the static field level was increased above a critical value, flux was driven irreversibly into the film at a field value such that the induced current density was $J_c\approx 2\times 10^6$ A/cm^2. While this value is smaller than the thermodynamic critical current, it is in agreement with experimental values for wide, flat samples.[12]

(iv) From a wide variety of experiments, we have shown that the results of the quadratic field dependence discussed in this paper are reproducible from film to film and are not affected by thermal cycling. The quadratic dependence was further shown to be not due to spurious effects such as leakage through the film. In addition, experiments with the films in a flux-induced state gave qualitatively different results and were not responsible for the results discussed in this paper.

The important aspect of these results, viz., the quadratic changes, both increases and decreases, of R_s are next examined in terms of microscopic theories. In particular, the task of a successful theory is a quantitative explanation of the experimental parameter $k(t,d)$ displayed in Figs. 5–7.

III. THEORY OF STATIC CURRENT EFFECTS ON SURFACE IMPEDANCE

A. General relations

The response of a superconductor to high-frequency fields is governed by the fundamental constitutive relation[13] between current $\mathbf{J}$ and vector potential $\mathbf{A}$. The relationship is local (wave vector $\mathbf{q}\to\mathbf{0}$) when the electronic mean free path $l<\xi_0$ (the bulk coherence length). In terms of the Mattis-Bardeen[14] complex conductivity $\tilde{\sigma}_s(\omega,T)=\sigma_1+i\sigma_2$, the J-A relation can be written

$$\mathbf{J}_\omega=(i\omega/c)\tilde{\sigma}_s(\omega,T)\mathbf{A}_\omega\ . \tag{3}$$

The real part of Eq. (3) represents the supercurrent response and the imaginary part, the "normal" or quasiparticle response.

In this paper, complex parameters are represented with a tilde, i.e., $\tilde{\sigma}$. All time dependences are taken to be $e^{-i\omega t}$. The complex surface impedance of very thin films can be written[15]

$$\tilde{Z}_s(d,\omega,T)\equiv R_s+iX_s=\frac{1}{\tilde{\sigma}_s d}=R_n(d)\left[\frac{\sigma_1}{\sigma_n}+\frac{i\sigma_2}{\sigma_n}\right]^{-1}, \tag{4}$$

where $R_n(d)=1/\sigma_n d$ is the normal state surface resistance and σ_n is the normal-state conductivity.

Adding a static current $\mathbf{J}_0$ shifts the total vector potential to $\mathbf{A}=\mathbf{A}_0+\mathbf{A}_\omega$. Expanding and retaining the first nonlinear term which is cubic in the total J-A relations, Eq. (3) is modified by an additional term which can be written

$$\delta\mathbf{J}_\omega=-2e^2D[\tilde{q}_1(\omega,t)(\mathbf{A}_0\cdot\mathbf{A}_0)\mathbf{A}_\omega+\tilde{q}_2(\omega,t)(\mathbf{A}_0\cdot\mathbf{A}_\omega)\mathbf{A}_0], \tag{5}$$

where $\tilde{q}_1,\tilde{q}_2$ are complex. It is assumed for generality that $\mathbf{A}_0$ and $\mathbf{A}_\omega$ can have arbitrary orientation in a two-dimensional plane.

Equation (5) describes the change in the high-frequency supercurrent and normal current due to the presence of a static current. The modifications are quadratic in the static current (since $\mathbf{J}_0\propto\mathbf{A}_0$) and are determined also by the relative orientation of static and high-frequency currents. Equation (5) may be interpreted as follows: the properties of the superconductor are modified by the presence of A_0 and A_ω due to a static perturbation ($\propto A_0^2$) and a dynamic perturbation ($\propto\mathbf{A}_0\cdot\mathbf{A}_\omega$). The first term represents a probe of the effects of the static perturbation by the high-frequency fields. The second term represents a mixing of the effects of the dynamic perturbation with the static current, which appears also at the driving frequency. The dynamic perturbation is absent if $\mathbf{A}_0$ and $\mathbf{A}_\omega$ are perpendicular to each other.

The conductivity represented by Eq. (5) is tensorial. However, we are only interested in the diagonal elements, the changes of which are

$$\delta\tilde{\sigma}_s\equiv\delta\sigma_1+i\delta\sigma_2=-\frac{2e^2DA_0^2}{i\omega}(\tilde{q}_1+\tilde{q}_2\cos^2\gamma), \tag{6}$$

where γ is the vector angle between $\mathbf{A}_0$ and $\mathbf{A}_\omega$. From Eq. (4), the normalized changes in impedance are

$$\frac{\delta R_s}{R_s}=\frac{\delta\sigma_1}{\sigma_1}-2\frac{\delta\sigma_2}{\sigma_2},\quad \frac{\delta X_s}{X_s}=-\frac{\delta\sigma_2}{\sigma_2}, \tag{7}$$

where we have assumed $\sigma_1\ll\sigma_2$, which applies to the present experiment. Equations (6) and (7) lead to

$$\frac{\delta R_s}{R_s}=\left[\frac{2e^2DA_0^2}{\omega}\right][P_1(\omega,t)+P_2(\omega,t)\cos^2\gamma], \tag{8}$$

where P_1 and P_2 are real quantities related to $\tilde{q}_1$ and $\tilde{q}_2$.

The above discussion is quite general, the only assumptions being that of local electrodynamics. To lowest order, the effect of J_0 is to change the impedance such that $\delta R_s,\delta X_s\propto J_0^2$, independent of J_ω. It is the task of a microscopic theory to yield the coefficients $\tilde{q}_1$ and $\tilde{q}_2$ (and, hence, P_1 and P_2), based upon a detailed examination of the processes involved. This is discussed next.

B. Microscopic theory

A complete description of a superconductor requires at least two components: the gap parameter and the quasiparticles, which are in general strongly intercoupled. These components are modified by perturbations such as external currents. In this work we have employed a microscopic formulation derived by Ovchinnikov and Schön[5,6] who describe such effects, and use the theory to calculate $\delta R_s/R_s$. In this section, a brief description of the physical processes is given, while a detailed discussion of the calculations is deferred to the Appendix.

The theory is applicable in the dirty limit $\tau_{el}T_c \ll 1$, where $\tau_{el}=l/v_F$ is the elastic scattering time. This should be valid for all the thin films described here. In the dirty limit, the effects of the superposed static and high-frequency currents are determined by a static pair-breaking parameter $\Gamma_0=2e^2DA_0^2$ and a dynamic pair-breaking parameter $\Gamma_\omega=2e^2D\mathbf{A}_0\cdot\mathbf{A}_\omega$. Note that Γ_ω is absent if $\mathbf{A}_0$ and $\mathbf{A}_\omega$ are orthogonal. The magnitude of the pair-breaking effects is determined by $\Gamma_0/\Delta(T)$ and $\Gamma_\omega/\Delta(T)$, where $\Delta(T)$ is the gap parameter. (We use units $k=\hbar=1$.)

Static pair-breaking effects due to a static current are well known;[13,16] the gap parameter Δ is decreased and the density of states is modified with introduction of states of minimum energy less than the zero current gap. This is shown in Fig. 8(a), where the dashed line is the zero-current BCS density of states and the solid line is the pair-breaking density of states $N(\Gamma_0,E)$. As a consequence, the total number N_{qp} of quasiparticles is increased, determined by

$$N_{qp}=\int N(\Gamma_0,E)f_{th}(E)dE\,,$$

where $f_{th}(E)$ is the equilibrium distribution function. Both these effects, viz., decreased Δ and increased N_{qp}, lead to decreased high-frequency supercurrent ($\delta\sigma_2<0$) and increased normal current ($\delta\sigma_1>0$). As a consequence, $\delta R_s>0$ and $\delta X_s>0$. The actual magnitude of these effects, which are represented by $\tilde{q}_1$ in Eq. (3) and P_1 in Eq. (8), requires numerical evaluation and is described in the Appendix.

The effect of the dynamic pair-breaking parameter Γ_ω is to cause oscillations of the gap parameter and of the density of states at the driving frequency ω. These components respond so long as $\omega<\Delta$, the gap frequency. Instantaneous "snapshots" of the oscillating density of states are shown in Fig. 8(b). The response of the quasiparticles on the other hand, is determined by an additional time scale—the inelastic quasiparticle scattering time τ_{in}. As discussed later in this section, τ_{in} can be quite long, and generally for $T<T_c$, $1/\tau_{in}<\Delta$, the gap frequency.

At low frequencies, $\omega<1/\tau_{in}$, the quasiparticle system responds adiabatically to the density-of-states oscillation. That is, the total quasiparticle number oscillates with the density of states, being determined instantaneously by the

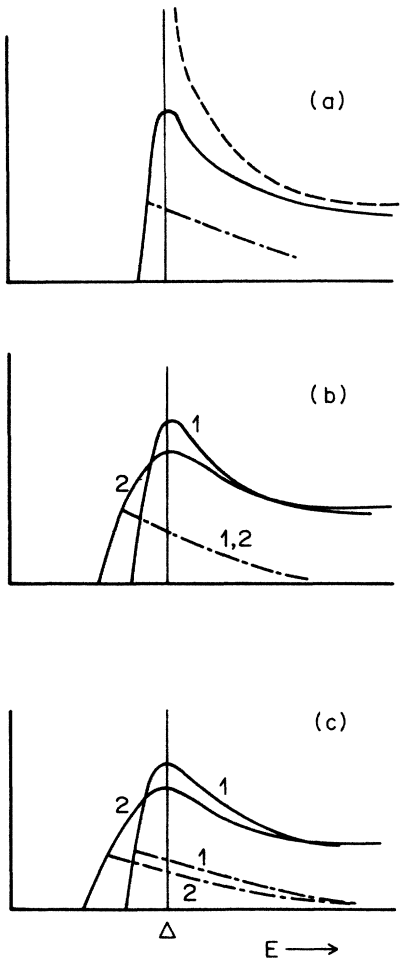

FIG. 8. Pair-breaking effects due to static and high-frequency currents in a dirty superconductor. (a) Density of states due to static pair-breaking parameter Γ_0 (solid line). The unperturbed BCS density of states (dashed line) is also shown. (b) and (c) Oscillating density of states (solid lines) and corresponding distribution functions (dashed-dotted lines) due to dynamic pairbreaking Γ_ω. At low frequencies $\omega\tau_{in}<1$ (b), the distribution function is unchanged from the thermal value, while at high frequency $\omega\tau_{in}\gg1$ (c), a counteroscillating component develops. The labels 1 and 2 refer to different instants during the microwave oscillation.

latter. In this adiabatic limit, the effect of Γ_ω is similar to Γ_0. The high-frequency supercurrent $\propto\Gamma_\omega A_0$ decreases and the normal current decreases. Thus, $\delta R_s,\delta X_s>0$.

In the high-frequency ($\omega\tau_{in}\gg1$) case, the density of states and order parameter still oscillate since their characteristic time scale is determined by Δ^{-1} ($<\omega^{-1}$). However, the total quasiparticle number cannot follow the field and remains constant. Instead the distribution function, $f(E)$ develops a nonthermal high-frequency oscillating component $f_\omega(E)$ whose equation of motion is given by the Boltzmann equation[6]

$$-i\omega N_1(E,\omega)f_\omega(E)=-\frac{i}{2}\left[\tanh\frac{E+\omega/2}{2T}-\tanh\frac{E-\omega/2}{2T}\right][\Delta_1(\omega)R_2(E,\omega)-4De^2\mathbf{A}_0\cdot\mathbf{A}_\omega N_2(E,\omega)R_2(E,\omega)]\,, \tag{9}$$

where N_1, N_2, R_1, R_2 are generalized densities of states[17] (see Appendix). It can be shown[6] that the total quasiparticle number $N_{qp} = \int f(E) N_1(E) dE$ does not respond, i.e., $dN_{qp}/dt = 0$, the total quasiparticle number does not adiabatically follow or "oscillate" with the field, though now the distribution function does, according to Eq. (9). This is shown pictorially in Fig. 8(c).

From Eq. (9) it will be seen that f_ω oscillates out of phase with A_ω. This counter oscillation leads to an *enhancement* of the high-frequency supercurrent. This becomes apparent by noting that the supercurrent $\mathbf{J}_s \propto [1-2f(\Delta)]\mathbf{A}$ so that

$$\delta J_{s\omega} \propto -[f_\omega A_0] \propto +[(\mathbf{A}_0 \cdot \mathbf{A}_\omega)\mathbf{A}_0] .$$

That is, if f decreases at the gap edge J_s increases. This supercurrent enhancement is equivalent to a decrease of the penetration depth—however, it must be emphasized that the observed decrease is really a dynamic oscillation of the penetration depth "sensed" by the static current. Finally, this is also equivalent to $\delta\sigma_2 > 0$ and hence $\delta R_s, \delta X_s < 0$. In addition, the "dissipative" normal current, driven by the electric field E_ω, is decreased. This again is equivalent to $\delta\sigma_1 < 0$ and again leads to $\delta R_s < 0$.

At any temperature, both the processes described above, viz., those due to Γ_0 which increase R_s and those due to Γ_ω which decrease R_s are operative. Numerical calculations are required to determine their magnitudes, and the details are described in the Appendix. The calculations show that near T_c, when $\Delta < T$, the static pair-breaking effects dominate, leading to $\delta R_s > 0$. At low temperatures when $\Delta > T$, the dynamic effects dominate, leading to an apparent enhancement of superconductivity ($\delta R_s < 0$). Comparison of theory to experiment is presented in the next section.

It is important to note the features of the present theory which depart significantly from earlier ideas. The static pair-breaking effects are derivable within a thermodynamic framework, according to which the gap parameter[18,19] and quasiparticle number are determined by the free energy associated with the current. Thermodynamics predicts only increases since the superconductor is "pushed" toward the normal state by the current. Indeed, as discussed later, the present calculations for $\tilde{q}_1$ do reduce to the Ginzburg-Landau[18] results near T_c. Regarding the dynamic pair-breaking effects, the adiabatic low-frequency effects should be similar, being determined by the instantaneous value of the total current.

Since the original arguments of Ginzburg, it has generally been believed that at high frequencies the dynamic effects should vanish when $\omega\tau_{in} > 1$, since the quasiparticle system cannot follow the field. This is usually represented as $\tilde{q}_2(\omega) \propto 1/(1+i\omega\tau_{in})$ and hence $P_2(\omega,t) \to 0$ as $\omega\tau_{in} \gg 1$. Thus, for all $\omega\tau_{in}, \delta R_s/R_s > 0$ according to previous arguments.

However, as discussed in this paper, an additional degree of freedom, viz., the quasiparticle distribution functions develops, in order to maintain a constant N_{qp}. This new distribution is of course nonthermal, and when included, yields a decrease of absorption. To reiterate, whereas a thermodynamic analysis yields only increases, a nonadiabatic or nonequilibrium analysis is required to describe the decrease of R_s or apparent enhancement of superconductivity.

The present form of the nonequilibrium theory is valid when $\omega\tau_{in} \gg 1$. The inelastic scattering rate that enters is the sum of rates of all relevant inelastic scattering processes. For the present situation, the dominant contributions arise from the inelastic quasiparticle phonon scattering rate $\tau_s(E)$ and the recombination rate $\tau_R(E)$. Thus, $1/\tau_{in} = 1/\tau_s + 1/\tau_R$. For quasiparticles near the gap edge $E \approx \Delta$, and at low temperatures ($\Delta \gg kT$), τ_s and τ_R can be written

$$\tau_s(\Delta,T) = \tau_0 \frac{1}{\Gamma(\frac{7}{2})\zeta(\frac{7}{2})} \left[\frac{2\Delta(0)}{kT}\right]^{1/2} \left[\frac{T_c}{T}\right]^{7/2}, \tag{10}$$

$$\tau_R(\Delta,T) = \tau_0 \frac{1}{\sqrt{\pi}} \left[\frac{kT_c}{2\Delta(0)}\right]^{5/2} \left[\frac{T_c}{T}\right]^{1/2} \exp(\Delta(0)/kT) . \tag{11}$$

Γ and ζ are the gamma and zeta functions, respectively, and τ_0 is a time characteristic of the material. For Sn, $\tau_0 = 2.3\times10^{-9}$ sec and for In, $\tau_0 = 7.8\times10^{-10}$ sec. In the temperature range $t > 0.4$, $\tau_s > \tau_R$ and hence recombination is the dominant relaxing channel. At 10 GHz, $\omega\tau_{in} \sim 50$ for Sn and hence the theory described above which is valid for $\omega\tau_{in} \gg 1$ should be applicable.

It is necessary to recast Eq. (8) in a form that allows comparison with the results of the present experiment. In this experiment (see Fig. 1), the static current is induced by applying a parallel magnetic field B_0 on only one side of the sample, with zero field on the other side, and is given by $J_0 = (c/4\pi)B_0/d$. The pair-breaking parameter $\Gamma_0 = 2De^2A_0^2 = \frac{2}{3}(\mathbf{p}_F \cdot \mathbf{v}_0)^2 l/v_F$ where p_F and v_F are the Fermi momentum and velocity, respectively, and

$$\mathbf{v}_0 = \mathbf{J}_0/n_s e = (4\pi e/mc^2)\lambda_l^2(t)J_0$$

is the induced velocity where $\lambda_l(t)$ is the MFP corrected penetration depth. In the dirty limit,

$$\lambda_l(t) = \lambda_p(t)(\xi_0/1.33l)^{1/2}$$
$$= \lambda_p(0)(\xi_0/1.33l)^{1/2}(1-t^4)^{-1},$$

where $\lambda_p(0)$ is the London penetration depth. Using also the result that when $v_0 = v_c(0)$ the critical velocity at $T = 0$ K, $P_F v_c(0) = \Delta(0) = e/mc\lambda_p(0)B_{c0}$, where B_{c0} is the bulk critical field at $T = 0$ K, Eq. (8) can be written

$$\frac{\delta R_s}{R_s} = \left[\frac{\alpha}{ld^2}\right] \frac{1}{(1-t^4)^2} [P_1(\omega,t)+P_2(\omega,t)]B_0^2$$
$$= k(\omega,t,d)B_0^2, \tag{12}$$

where $\alpha = \frac{2}{3}(\lambda_p^2\xi_0/B_{c0}^2)\Delta(0)$ is a quantity characteristic of the pure bulk material. In the present experiment, the angle $\gamma = 0$.

Thus, the theory, which yields the quadratic dependence for $\delta R_s/R_s$ on the current-inducing field, predicts a universal material-independent behavior

$$[P_1(\omega,t)+P_2(\omega,t)]/(1-t^4)^2$$

for the quadratic coefficient k as a function of ω and t, with a scale factor α/ld^2 determined by material parameters.

IV. DISCUSSION

The theory described in the last section, whose central feature is a nonthermal response of the quasiparticles, yields [Eq. (12)] the quadratic dependence on current-inducing field, observed in the experiments. In this section, we compare the calculated coefficient $k(\omega,t,d)$ with the experimental coefficient $k(t,d)$ measured at 10 GHz.

The theory is strictly valid where local electrodynamics is applicable, and where the inelastic scattering rate is slow so that $\omega\tau_{\rm in}\gg 1$ at the measuring frequency. These criteria should be met (as discussed previously) in very thin Sn films at 10 GHz.

In Fig. 5, the calculated quadratic coefficients $k(\omega,t,d)$ in Eq. (12) for two films of Sn with $d=260$ and 500 Å are displayed as solid lines, along with experimental data. The method of calculating the functions P_1 and P_2 is discussed in the Appendix. For Sn, the values $\lambda_p=510$ Å, $\xi_0=2300$ Å, and $B_{c0}=330$ G reported in the literature were used. Note that $\omega=2\pi\times 1.012\times 10^9$/sec, and l and d were measured as discussed in Sec. I. There are thus no adjustable parameters in the comparison

From Fig. 5, it will be seen that theory and experiment agree extremely well, in regard to both temperature and thickness dependence, within the experimental accuracy for these very thin Sn films. The theory yields the experimentally observed high-temperature increase and low-temperature decrease of R_s, both qualitatively and quantitatively. The excellent agreement leads to the conclusion that the physical processes discussed in Sec. III, viz., the order parameter depression at high temperature leading to $\delta R_s>0$ and the low-temperature enhancement of supercurrent and decrease of normal current due to a nonthermal distribution function, were operant in these films.

We have also compared the experimental results with the Ginzburg-Landau[18] (GL) thermodynamic theory. The latter yields

$$k_{\rm GL}(t,d)=\left[\frac{\lambda_l(0)}{d}\right]^2\frac{1}{B_{c0}^2}\,\frac{1}{(1-t^2)^2(1-t^4)}\,, \qquad (13)$$

with $k_{\rm GL}>0$ for all t. Very near T_c, Eq. (13) does agree with the experimental results and with Eq. (12). However, it is apparent that as T is lowered, the quasiparticle effects become increasingly important. Even in the temperature region $0.9<t<0.95$, where $k(t,d)>0$, the nonequilibrium theory Eq. (12) gives better agreement than Eq. (13). For $t<0.88$, $k(t,d)<0$ and Eq. (13) disagrees even qualitatively regarding the sign. Thus, the nonequilibrium theory provides an excellent description of the results over a wide temperature range, while the equilibrium GL theory is valid only near T_c.

We have also done experiments in a regime where local electrodynamics becomes invalid. From those experiments, we can determine the importance of the assumption of locality which is built into our theory. These experiments have been done by measuring $k(t,d)$ for thicker Sn films ($d=800$, 1000, and 2000 Å). For these films, the high-temperature ($0.9<T<0.98$) results were found to be in reasonable agreement with the GL results Eq. (13). Thus, at these high temperatures, the depression of the order parameter was being observed. However, it was found that $\delta R_s>0$ at lower temperature also, in contrast to the thick-film results where $\delta R_s<0$ for $t\lesssim 0.88$. Even in these thicker films, the dirty-limit theory should apply since $\tau_{\rm el}\Delta\ll 1$. Furthermore, $\omega\tau_{\rm in}\gg 1$ also and the quasiparticles should be out of equilibrium. However, an important assumption—that the static and high-frequency currents are spatially uniform (allowing the wave-vector $\mathbf{q}\to\mathbf{0}$ limit)—is no longer valid. For the thicker films, the currents are not uniform. Also, the local limit wherein the current and vector potential are related [Eqs. (3) and (5)] at a point is also invalid. Independent evidence for this assertion comes from examining the surface resistance $R_s(0)$ in the absence of static current. In particular, the thickness dependence of $R_s(0)$ is not simply that predicted by Eq. (4). Rather, a nonlocal generalization of the linear Eq. (3) has to be used. This means that the local ($\mathbf{q}\to\mathbf{0}$) relation Eq. (5) does not apply but that spatial averages have to be included. Such spatial averages could introduce current contributions in addition to the purely local effects discussed in this paper. In other words, the present analysis, which is purely local and temporal, seems in need of generalization to include space and time effects, in order to correctly describe the results for thicker films.

We have also measured $k(t,d)$ for In films with $d=500$ and 1000 Å. The results for $d=500$ Å are displayed in Fig. 7 (the $d=1000$-Å results are similar). The results are qualitatively similar to those for the thinner Sn films, viz., a high-temperature increase ($k>0$) and a low-temperature decrease ($k<0$). However, an important difference is the temperature (between 0.58 and 0.65) at which k changes sign, compared to ≈ 0.88 for the thin Sn films. The nonequilibrium theory yields a universal curve for the t dependence, independent of material, and is shown also as the solid line. Comparison with Eq. (13) (the dashed line) indicates, that for the In films, quasiparticle effects are more important in In at temperatures lower than those for Sn. This may arise from the shorter (by 5) inelastic scattering rate in In. The present nonequilibrium theory is valid when $\omega\tau_{\rm in}\gg 1$, a limit that should be more valid in Sn. Since $\tau_{\rm in}$ gets larger with decreasing temperature, the present theory may be expected to show better agreement at lower temperatures, and Fig. 5 does indeed suggest this. Thus, we believe that inclusion of finite $\omega\tau_{\rm in}$ would explain the detailed temperature dependence for In.

To summarize this discussion, the present nonequilibrium theory describes very well the novel results for very thin Sn films, where the approximations for local electrodynamics and large inelastic scattering rate are valid. Further extensions to nonlocal electrodynamics and finite inelastic scattering rate are required to explain the results for the thicker Sn films and the In films.

V. COMMENTS

In this section, the significance of the present results in relation to earlier similar experiments and to current ideas of nonequilibrium superconductivity is examined.

A. Earlier experiments on $R_s(B_0)$

The experiment described here falls in the same class as similar experiments[1,2,20,21] carried out in the last 25 years to examine the static magnetic field dependence of the microwave impedance of bulk superconductors. While decreases in $R_s(B_0)$ were observed in the bulk experiments, they were complicated functions of temperature, frequency, orientation, etc., and a satisfactory solution was never found.

The present experiment has two significant and advantageous features in relation to the early bulk experiments, which greatly facilitate analysis. One is the enormous improvement in sensitivity which allows the study of effects due to small static current. The other is the ability to vary film thickness, which allows the considerable manipulation of material parameters.

The use of a fully superconducting cavity in which the film dominates the absorption enables us to achieve sensitivity orders of magnitude better than achieved before. We are able to measure $\delta R_s/R_s \sim 10^{-5}$ (*at low temperature,* $\delta R_s \sim 10^{-9}$ Ω/sq). The sensitivity of the bulk experiments was $\delta R_s/R_n \sim 10^{-4}$. Since $R_s/R_n \sim 10^{-3}$ at low temperature, we see that the lower limit on the sensitivity is 10^{-8} better in the present than in the previous experiments. The advantage of this increased sensitivity is that it allows the study of very small perturbations ($B_0/B_{c0} \sim 10^{-2}-10^{-3}$). At these low perturbations, $\mathbf{p}_F \cdot \mathbf{v}_0 \ll \omega, T, \Delta$—an important limit for the relevant theories. In the bulk experiments, to date, the fields are comparable to the critical field so that typically $\mathbf{p}_F \cdot \mathbf{v}_0 \gg \omega, T$, which greatly complicates the analysis. In particular, it is not clear if quadratic behavior was always observed. In any case, the quadratic coefficient was never explicitly evaluated. We believe that the understanding of similar experiments performed to date has been hampered by the high fields that were used. Indeed, there is experimental and theoretical evidence (see Appendix) that supports this assertion.

The second aspect concerns the ability to vary film thickness, which allows us to explore the wave-vector dependence of the superconductor-electromagnetic interaction and the effects of scattering. The bulk experiments did not have this flexibility since they were mostly confined to the case of large q (pure type-I superconductors). This, together with the spatial inhomogeneity of the fields, would lead to complications in the analysis for those experiments.

Keeping the above cautionary statements in mind, it is necessary to remark on one significant aspect of the present thin-film data in relation to earlier experiments on bulk. In the bulk experiments, it has been generally found that

$\delta R_s < 0$, $t \geq 0.9$ (≥ 0.7 in some cases),

$\delta R_s > 0$ at lower temperature .

Thus, the bulk results and the present thin-film results appear orthogonal as far as the T dependence of the sign of δR_s is concerned. However, Richards[22] found that in bulk Sn doped with In, $\delta R_s > 0$ for $0.3 < t < 0.98$, similar to our data on thicker films. Thus, there seems to be a continuous transition from dirty thin films to clean bulk, with the present thicker films and Sn doped with In, representing intermediate situations.

Boundaries and impurities strongly affect the elastic scattering MFP and hence tend to make the electrodynamics more local. Furthermore, in the bulk the current distributions are spatially inhomogeneous and nonlocal effects are more important. In the light of the above discussion, the present analysis indicates that spatial nonlocal effects would play an increasingly important role. Furthermore, since $\omega\tau_{in} \gg 1$ in bulk also, it seems necessary to carry out a nonequilibrium calculation including nonlocal effects in order to explain the bulk results. To date, no such analysis has been carried out, while all other analyses have failed to explain the results, particularly in the parallel-fields case, where, as we have discussed in Sec. III, nonequilibrium effects are particularly important.

B. Nonequilibrium superconductivity

Recently there has been intense interest[8] in nonequilibrium situations in superconductors induced by external perturbations. The essential description of such phenomena involves[17] a nonthermal quasiparticle distribution function $f^*(\varepsilon_k)$ that is different from the equilibrium or thermal Fermi distribution, $f_{th}(\varepsilon_k)$, and is determined by the strength and nature of the driving perturbation. ε_k is the energy of a quasiparticle of momentum $\mathbf{k}$. It is possible to classify nonequilibrium phenomena into two broad categories determined by $f^*(\varepsilon_k)$. Situations where $f^*(\varepsilon_k)$ is odd in ε_k are referred to as the odd or transverse T mode. Branch imbalance and thermoelectric phenomena fall under this class.

Microwave radiation produces an $f^*(\varepsilon_k)$ which is even in ε_k, and this mode is referred to as the even or longitudinal L mode. Microwave enhancement of the gap and critical current are examples of L-mode situations. However, in those experiments, the distribution and its consequences are determined by the strength of the driving microwave field B_ω, i.e., $f^*(\varepsilon_k) - f(\varepsilon_k) \propto B_\omega^2$, and the enhancement effects[23] are also $\propto B_\omega^2$. In this case, f^* is a steady-state quantity and is time independent.

The nonequilibrium f_ω discussed in this work can be associated with the L mode. However, a fundamental difference with other enhancement experiments is that $f_\omega \propto B_0 B_\omega$ and is time dependent. The enhancement observed in this work is the enhancement of high-frequency supercurrent due to the presence of static current. The high-frequency normal current is also reduced. The high-frequency response is still linear and the measured quantities, e.g., δR_s are independent of B_ω.

The only other experiment that is similar to the present work is that of Peters and Meissner,[24] which was carried out at lower frequencies (up to 1 GHz) and near T_c. Those authors were able to explain most of their results by

a simple relaxational extension[25] of the Ginzburg-Landau theory, viz., $\delta\sigma(\omega)=(\delta\sigma_2)_{\rm GL}1/1+i\omega\tau_{\rm in}$, where $(\delta\sigma_2)_{\rm GL}$ is obtained from the GL theory. However, at high frequencies and as temperature was lowered, they observed an excess conductivity above that given by the above expression. This excess conductivity[26] has never been explained. However, the present analysis gives a qualitative explanation. When $\omega\tau_{\rm in}>1$, the counteroscillating f_ω gives an enhanced supercurrent and hence $\delta\sigma_2$ is increased. Quantitative comparison requires extension of the present theory for $\omega\tau_{\rm in}\sim 1$.

CONCLUSIONS

The unusual results of the present experiments and the analysis of the quasiparticle response clearly demonstrate that superconductors are driven out of equilibrium in the presence of high-frequency radiation. In particular, these results demonstrate that nonequilibrium effects in superconductors can even be induced by vanishingly small microwave radiation if in the presence of a static current. The dynamic quasiparticle response, which we have described in terms of a time-dependent distribution function, manifests itself as an apparent enhancement of superconductivity. The analysis presented here quantitatively describes the experimental results that were observed in very thin Sn films, where the assumptions of the theory are valid. The experiments on the thickness dependence indicate that nonlocal effects will be important in bulk superconductors.

ACKNOWLEDGMENTS

We thank G. J. Dick for extensive discussions and comments. Invaluable technical assistance was provided by Edward Boud. J. M. Greif supplied many of the data acquisition programs and Dave Bell provided valuable advice in construction of the electronics. We are grateful to Gerd Schön for his time and patience during extensive discussions regarding the theory. This work was supported by the National Science Foundation under Grant No. PHY-80-15508A01.

APPENDIX

1. Calculation of high-frequency response of thin "dirty" films in the presence of a static current

In this appendix we summarize the relations used to calculate the changes in the surface impedance of a thin "dirty" film caused due to a static current flowing in the film.

Associated with the static $\mathbf{J}_0$ and high-frequency $\mathbf{J}_\omega$ ($\ll\mathbf{J}_0$) are vector potentials $\mathbf{A}_0$ and $\mathbf{A}_\omega$ ($\ll\mathbf{A}_0$). The high-frequency part of the current-vector potential relation can be written[5,6]

$$\frac{\mathbf{J}_\omega}{\sigma_n}=-\tilde{Q}_1(\omega,\Gamma_0,t)\mathbf{A}_\omega-2e^2D\frac{(\mathbf{A}_0\cdot\mathbf{A}_\omega)}{\omega}\tilde{Q}_2(\omega,\Gamma_0,t)\mathbf{A}_0, \tag{A1}$$

where σ_n is the normal-state conductivity and $\Gamma_0=2e^2DA_0^2$ is the pair-breaking parameter. Equation (A1) includes effects to all order in Γ_0 ($<\Delta$). In contrast, Eq. (5) retains only effects linear in Γ_0, which is the limit relevant to the present work. Comparing

$$2e^2D\tilde{q}_1=\Gamma_0\left[\frac{\tilde{Q}_1(\Gamma_0)-\tilde{Q}_1(0)}{\Gamma_0}\right]_{\Gamma_0=0},$$
$$2e^2D\tilde{q}_2=\Gamma_0\tilde{Q}_2(\omega,\Gamma_0=0).$$

In general, we are interested in the components of $\mathbf{J}_\omega$ along $\mathbf{A}_\omega$. Dropping vector notation,

$$\frac{J_\omega}{\sigma_n}=-\left[\tilde{Q}_1(\omega,\Gamma_0,T)+\frac{\Gamma_0}{\omega}\cos^2\gamma\tilde{Q}_2(\omega,\Gamma_0,T)\right]A_\omega, \tag{A2}$$

where γ is the angle between $\mathbf{A}_0$ and $\mathbf{A}_\omega$.

This expression may be written in the Mattis-Bardeen[17] form, $J_\omega=\tilde{\sigma}_sE_\omega=i\omega\tilde{\sigma}_sA_\omega$ (the convention is that oscillating quantities are $\propto e^{-i\omega t}$). Then

$$\frac{\tilde{\sigma}_s}{\sigma_n}=\frac{i}{\omega}\left[\tilde{Q}_1+\left[\frac{\Gamma_0}{\omega}\right](\cos^2\gamma)\tilde{Q}_2\right]$$
$$=\left[\frac{\sigma_1}{\sigma_n}\right]+i\left[\frac{\sigma_2}{\sigma_n}\right], \tag{A3}$$

where

$$\left[\frac{\sigma_1}{\sigma_n}\right]=-\frac{1}{\omega}\,\mathrm{Im}\tilde{Q}_1(\omega,T,\Gamma_0)$$
$$-\left[\frac{\Gamma_0}{\omega^2}\right]\mathrm{Im}\tilde{Q}_2(\omega,T,\Gamma_0)\cos^2\gamma$$
$$=\left[\frac{\sigma_{11}}{\sigma_n}\right]+\left[\frac{\delta\sigma_{12}}{\sigma_n}\right]\cos^2\gamma, \tag{A4}$$

$$\left[\frac{\sigma_2}{\sigma_n}\right]=\frac{1}{\omega}\,\mathrm{Re}\tilde{Q}_1(\omega,T,\Gamma_0)+\left[\frac{\Gamma_0}{\omega^2}\right]\mathrm{Re}\tilde{Q}_2(\omega,T,\Gamma_0)\cos^2\gamma$$
$$=\left[\frac{\sigma_{21}}{\sigma_n}\right]+\left[\frac{\delta\sigma_{22}}{\sigma_n}\right]\cos^2\gamma. \tag{A5}$$

It should be noted that the Mattis-Bardeen results (called σ_{10},σ_{20}) are a special case of equations (A4) and (A5) (with $\Gamma_0=0$):

$$\frac{\sigma_{10}}{\sigma_n}=-\frac{1}{\omega}\,\mathrm{Im}\tilde{Q}_1(\omega,T,\Gamma_0=0),$$
$$\frac{\sigma_{20}}{\sigma_n}=\frac{1}{\omega}\,\mathrm{Re}\tilde{Q}_1(\omega,T,\Gamma_0=0). \tag{A6}$$

The relative changes in the conductivity can be written as

$$\frac{\delta\sigma_1}{\sigma_{10}}=\frac{\sigma_1-\sigma_{10}}{\sigma_{10}}=\frac{[\sigma_{11}(\Gamma_0)-\sigma_{10}]+\delta\sigma_{12}\cos^2\gamma}{\sigma_{10}}$$
$$=\frac{\delta\sigma_{11}+\delta\sigma_{12}\cos^2\gamma}{\sigma_{10}}, \tag{A7}$$

$$\frac{\delta\sigma_2}{\sigma_{20}}=\frac{\sigma_2-\sigma_{20}}{\sigma_{20}}=\frac{[\sigma_{21}(\Gamma_0)-\sigma_{20}]+\delta\sigma_{22}\cos^2\gamma}{\sigma_{20}}$$
$$=\frac{\delta\sigma_{21}+\delta\sigma_{22}\cos^2\gamma}{\sigma_{20}}\ . \tag{A8}$$

For the special cases of parallel and perpendicular fields, the relative changes in conductivity can be written

$$\frac{\delta\sigma_{1\perp}}{\sigma_{10}}=\frac{\delta\sigma_{11}}{\sigma_{10}},\quad \frac{\delta\sigma_{2\perp}}{\sigma_{20}}=\frac{\delta\sigma_{21}}{\sigma_{20}}\quad \text{for } \gamma=\pi/2, \tag{A9}$$

$$\frac{\delta\sigma_{1\parallel}}{\sigma_{10}}=\frac{\delta\sigma_{11}+\delta_{12}}{\sigma_{10}},\quad \frac{\delta\sigma_{2\parallel}}{\sigma_{20}}=\frac{(\delta\sigma_{21}+\delta\sigma_{22})}{\sigma_{20}}\quad \text{for } \gamma=0\ . \tag{A10}$$

Finally we restate the equations that lead to the changes in the surface resistance in the local thin-film limit:

$$\frac{\delta R_s}{R_s}=\frac{\delta\sigma_1}{\sigma_1}-2\frac{\delta\sigma_2}{\sigma_2},\quad \frac{\delta X_s}{X_s}=-\frac{\delta\sigma_2}{\sigma_2}\ . \tag{A11}$$

2. Calculation of Q_1 and Q_2 and $\sigma_1/\sigma_n,\sigma_2/\sigma_n$

The evaluation of detailed expressions for the kernels Q_1 and Q_2, using thermal Green's-function techniques, has been carried out in Refs. 5 and 6. The theory applies to uniform currents (in static and high-frequency, wave-vector limit $\mathbf{q}\to\mathbf{0}$) and where $1/\tau_{\rm in}\to\infty$, so that level broadening due to the electron-phonon interaction may be neglected. Here we present the relations which lead to numerical calculations for the effects of a static current on the impedance.

In the presence of a pair-breaking perturbation, generalized densities of states, N_1,R_1,N_2,R_2 may be introduced[27] which are expressible in terms of retarded Green's functions $\tilde{g}(E)$ and $\tilde{F}(E)$:

$$N_1(E)=\mathrm{Re}\tilde{g},\quad R_1(E)=\mathrm{Im}(\tilde{g}),\quad R_2(E)=\mathrm{Re}(\tilde{F}),$$
$$N_2(E)=-\mathrm{Im}\tilde{F},$$

where $\tilde{g}$ and $\tilde{F}$ satisfy

$$\tilde{g}^2-\tilde{F}^2=1, \tag{A12a}$$

$$\Delta\tilde{g}-(E+i0)\tilde{F}=i\Gamma\tilde{g}\tilde{F}, \tag{A12b}$$

where $\Delta(T,\Gamma_0)$ is the new order parameter in the presence of pair-breaking. The dependence of $\Delta(T,\Gamma_0)$ was approximated by the form[27]

$$\Delta(T,\Gamma_0)=1-\left[\frac{\Gamma_0}{\Delta}\right]\left[\frac{\pi^2}{8}\right]\frac{\mathcal{N}}{\mathcal{D}}, \tag{A13a}$$

$$\mathcal{N}=\tanh\left[\frac{\Delta}{2T}\right]+\left[\frac{\Delta}{2T}\right]\mathrm{sech}^2\left[\frac{\Delta}{2T}\right], \tag{A13b}$$

$$\mathcal{D}=\sum_{n=0}^{\infty}\frac{1}{[(2n+1)^2+(\Delta/\pi T)^2]^{5/2}}\ .$$

Equations (A12) and (A13) are well known in the theory of pair-breaking effects.[16]

We define normalized quantities:

$$\bar{E}=E/\Delta(T,\Gamma_0),\quad \bar{\Gamma}_0=\Gamma_0/\Delta(T,\Gamma_0)\ .$$

Combining Eq. (A10) and (A11) and substituting $g=ih$,

$$\bar{\Gamma}_0^2h^4-2\bar{E}\,\bar{\Gamma}_0h^3+[\bar{E}^2+(\bar{\Gamma}_0^2-1)]h^2-2\bar{E}\,\bar{\Gamma}_0h+\bar{E}^2=0\ . \tag{A14}$$

There exists a minimum excitation energy value $\bar{\Omega}_G$ (the new gap): $\bar{\Omega}_G=(1-\bar{\Gamma}_0^{2/2})^{3/2}$. Of the four roots of Eq. (A14), the following were chosen in accordance with the requirement that as $\Gamma_0\to0$, the generalized densities of states should reduce to their BCS form.

(1) $\bar{E}\geq\bar{\Omega}_G$: *Complex roots with* $\mathrm{Im}(\tilde{h})=-\mathrm{Re}(\tilde{g})<0$.

(2) $\bar{E}\leq\bar{\Omega}_G$: *Real root with* (a) $\mathrm{Re}\tilde{h}<0$ or (b) $\mathrm{Re}\tilde{h}\to0$ as $\bar{E}\to0$.

Expressions for the conductivities σ_{11} and σ_{21} are

$$\frac{\sigma_{11}}{\sigma_n}=\frac{2}{\omega}\int_{\bar{\Omega}_G}^{\infty}d\bar{E}[N_1(\bar{E})N_1(\bar{E}+\bar{\omega})+R(\bar{E})R_2(\bar{E}+\bar{\omega})]$$
$$\times[f(\bar{E}-f(\bar{E}+\bar{\omega})], \tag{A15}$$

where

$$f(E)=\left[\exp\left[\frac{E}{T}\right]+1\right]^{-1}, \tag{A16}$$

$$\frac{\sigma_{21}}{\sigma_n}=\frac{1}{2\bar{\omega}}\left[\int_{\bar{\Omega}_G-\bar{\omega}}^{\infty}d\bar{E}\left[\tanh\left[\frac{\bar{E}+\bar{\omega}}{2T}\right]+\tanh\left[\frac{\bar{E}}{2T}\right]\right]\right.$$
$$\times[N_2(\bar{E})R_2(\bar{E}+\bar{\omega})-N_1(\bar{E}+\bar{\omega})R_1(\bar{E})]$$
$$\left.\times\int_{\bar{\Omega}_G}^{\infty}d\bar{E}\left[\tanh\left[\frac{\bar{E}-\bar{\omega}}{2T}\right]+\tanh\left[\frac{\bar{E}}{2T}\right]\right]\right.$$
$$\times[N_2(\bar{E})R_2(\bar{E}-\bar{\omega})-N_1(\bar{E}-\bar{\omega})R_1(\bar{E})]\ .$$

To summarize the procedure: A given value of $\Gamma_0/\Delta(T,0)$ (typically <0.3) was input to the numerical program. $\Delta(T,\Gamma_0)$ was calculated using Eq. (A13) and also the normalized quantities $\bar{\Gamma}_0$, $\bar{\Omega}_G$, and $\bar{\omega}$. The generalized densities of states were computed using the procedure outlined and Eqs. (A13) and (A14) used to calculate the Γ_0-dependent conductivities.

The numerical evaluation of σ_1 and σ_2 in the limit $\Gamma_0=0$ (i.e., the Mattis-Bardeen conductivities σ_{10} and σ_{20}) using Eqs. (A15) and (A16) is almost impossible due to the appearance of singularities in generalized densities of states. Instead we used the well-known forms[17]

$$\sigma_{10}=\frac{2}{\omega}\int_{\Delta}^{\infty}dE[f(E)-f(E+\omega)] \times\frac{(E^2+\Delta^2+\omega E)}{(E^2-\Delta^2)^{1/2}[(E+\omega)^2-\Delta^2]^{1/2}}, \quad \text{(A17)}$$

$$\sigma_2=\frac{1}{\omega}\int_{\Delta-\omega}^{\Delta}dE[1-2f(E+\omega)]\frac{(E^2+\Delta^2+\omega E)}{[(E+\omega)^2-\Delta^2]^{1/2}}. \quad \text{(A18)}$$

For small $\Gamma_0\ll\Delta(T)$, numerical calculations show that the changes in conductivity $\delta\sigma_{11}$ and $\delta\sigma_{21}$, calculated from Eq. (A10) using Eqs. (A15)–(A18), are linear in Γ_0 (and hence quadratic in B_0).

3. Calculation of $\delta\sigma_{12}$ and $\delta\sigma_{22}$ to order Γ

When the static and high-frequency currents are not perpendicular, additional contributions enter due to the Q_2 kernel, which are essentially nonequilibrium contributions. We restrict these considerations to the limit of effects linear in Γ_0 (i.e., A_0^2). Then it is sufficient to calculate $Q_2(\omega,T,\Gamma_0=0)$, as is evident from Eqs. (A4) and (A5):

$$\delta\frac{\sigma_{12}}{\sigma_n}=-\left[\frac{\Gamma_0}{\Delta}\right]\left[\frac{\Delta}{\omega}\right]\frac{\mathrm{Im}\tilde{Q}_2(\omega,T,\Gamma_0=0)}{\omega}, \quad \text{(A19)}$$

$$\delta\frac{\sigma_{22}}{\sigma_n}=+\left[\frac{\Gamma_0}{\Delta}\right]\left[\frac{\Delta}{\omega}\right]\frac{\mathrm{Re}\tilde{Q}_2(\omega,T,\Gamma_0=0)}{\omega}. \quad \text{(A20)}$$

From Ref. 6, $\tilde{Q}_2=\tilde{I}_2+\tilde{I}_2^2/\omega\tilde{I}_3$, where $\tilde{I}_1$, $\tilde{I}_2$, and $\tilde{I}_3$ are integrals. For $\omega<2\Delta$, $\tilde{I}_3=-2$ exactly. Hence,

$$\left[\frac{\delta\sigma_{12}}{\sigma_n}\right]=-\left[\frac{\Gamma_0}{\Delta}\right]\left[\frac{\Delta}{\omega}\right]\left[\frac{\mathrm{Im}\tilde{I}_2}{\omega}-\left[\frac{\mathrm{Re}\tilde{I}_1}{\omega}\right]\left[\frac{\mathrm{Im}\tilde{I}_1}{\omega}\right]\right]_{\Gamma_0=0}, \quad \text{(A21)}$$

$$\left[\frac{\delta\sigma_{22}}{\sigma_n}\right]=+\left[\frac{\Gamma_0}{\Delta}\right]\left[\frac{\Delta}{\omega}\right]\times\left\{\frac{\mathrm{Re}\tilde{I}_2}{\omega}-\frac{1}{2}\left[\left[\frac{\mathrm{Re}\tilde{I}_1}{\omega}\right]^2-\left[\frac{\mathrm{Im}\tilde{I}_1}{\omega}\right]^2\right]\right\}_{\Gamma_0=0}. \quad \text{(A22)}$$

The integrals I_1 and I_2 are expressible as follows in the limit $\Gamma_0=0$ [$b=\omega/\Delta(T)$, $y=E/\Delta(T)$]:

$$\frac{\mathrm{Im}\tilde{I}_2}{\omega}=\frac{2\pi}{b}[f(\Delta)-f(\Delta+\omega)]\frac{1+b}{(2b+b^2)^{1/2}},$$

$$\frac{\mathrm{Re}\tilde{I}_2}{\omega}=\frac{\pi}{b}\tanh\left[\frac{\Delta}{2T}\right]\frac{1-b}{\sqrt{2b-b^2}},$$

$$\frac{\mathrm{Re}\tilde{I}_1}{\omega}=2\int_1^{1+b}dy\tanh\left[y\frac{\Delta}{2T}\right]\times\frac{1}{\{[1-(y-b)^2](y^2-1)\}^{1/2}},$$

$$\frac{\mathrm{Im}\tilde{I}_1}{\omega}=2\int_1^{\infty}dz\left[\tanh\left[y\frac{\Delta}{2T}\right]-\tanh\left[(y+b)\frac{\Delta}{2T}\right]\right]\times\frac{1}{\{[(y+b)^2-1](y^2-1)\}^{1/2}}.$$

It is useful to state the low-temperature limit ($T\ll\Delta$) of the above expressions:

$$\frac{\sigma_{10}}{\sigma_n}\approx\left[\frac{2\Delta}{T}\right]\left[\ln\left[\frac{4T}{\omega}\right]-\gamma\right]e^{-\Delta/T},\quad \frac{\sigma_{20}}{\sigma_n}\approx\frac{\pi}{b},$$

$$\frac{\delta\sigma_{12}}{\sigma_{10}}\approx-\left[\frac{\Gamma}{\Delta}\right]\left[\frac{\pi}{\sqrt{2}}\frac{1}{b^{3/2}}\frac{1}{[\ln(4T/\omega)-\gamma]}+\pi\right],$$

$$\frac{\delta\sigma_{22}}{\sigma_{20}}\approx\left[\frac{\Gamma}{\Delta}\right]\left[\frac{1}{\sqrt{2}}\frac{1}{b^{3/2}}-\frac{\pi}{2}\right].$$

It is interesting that $\delta\sigma_{12(22)}/\sigma_{10(20)}\propto(\Delta/\omega)^{3/2}$. This is only true so long as $\omega\tau_{\mathrm{in}}\gg1$. Thus, this dynamical theory does not reduce smoothly to the quasistatic or adiabatic limit.

At high fields, where $\Gamma_0^{2/3}>\omega$ ($\Delta>\Gamma_0$), the calculations show that δR_s can decrease due to an interesting effect.[3] In the absence of a static current, $R_s\propto\omega^2\ln(8\Delta/\omega)e^{-\Delta/T}$ at low temperature.[4] The ln term arises[13] due to the BCS singularity in the density of states. In the presence of a pair-breaking perturbation this singularity is smoothed out.[13,16] As a consequence, the ln term is modified and, more importantly, reduced in magnitude; depending on the temperature and the value of Γ, this decrease can counteract the increase due to the depression of the gap, resulting in a decreased adsorption. Interestingly the present results for the case of perpendicular fields are similar to those calculated by Garfunkel[20] in the "clean" bulk case with the additional assumption (by Garfunkel) of diffuse reflection for electrons at the surface.

In the model of Garfunkel, $\delta R_s<0$ for $p_F v_0>\omega$ and $\delta R_s>0$ for $p_F v_0<\omega$, where p_F is the Fermi momentum and v_0 the velocity due to the supercurrent. The decrease at large velocities is essentially due to a modification of the density of states. Raynes[28] has found agreement with his experimental results on clean bulk Al, for the case of perpendicular fields. It is important to emphasize that the above is a high-field effect, unlike the decrease observed in the present experiment at very low currents where $p_F v_0\ll\omega$.

*Present address: Department of Physics, University of California, Los Angeles, CA 90024.

[1]A. B. Pippard, Proc. R. Soc. London, Ser. A **203**, 210 (1950); Adv. in Electron Phys.

[2]A. B. Pippard, in *Superconductor Applications: SQUIDS and Machines,* Vol. 21 of *NATO Advanced Study Institute Series,* edited by B. B. Schwartz and S. Foner (Plenum, New York, 1977). For a guide to the earlier literature, see also B. D. Josephson, J. Phys. F **4**, 751 (1974).

[3]S. Sridhar and J. E. Mercereau, Bull. Am. Phys. Soc. **28**, 465 (1983).

[4]S. Sridhar, Ph.D. thesis, California Institute of Technology, 1983.

[5]Yu. N. Ovchinnikov, Zh. Eksp. Teor. Fiz. **59**, 128 (1971) [Sov. Phys.—JETP **32**, 72 (1971)].

[6]Y. N. Ovchinnikov and Gerd Schön (unpublished).

[7]S. B. Kaplan, C. C. Chi, D. N. Langenberg, J. J. Chang, S. Jafarey, and D. J. Scalapino, Phys. Rev. B **14**, 4854 (1977).

[8]*Nonequilibrium Superconductivity, Phonons and Kapitza Boundaries,* Vol. 65 of *NATO Advanced Studies Institutes Series,* edited by K. E. Gray (Plenum, New York, 1982).

[9]A. Schmid and Gerd Schön, J. Low Temp. Phys. **20**, 207 (1975). The oscillating part of the distribution function in the present paper corresponds to the L mode of these authors.

[10]J. E. Mooij, in Ref. 8, Chap. 7.

[11]D. C. Larson, in *Physics of Thin Films* (Academic, New York, 1971), Vol. 6.

[12]J. A. Mydosh and H. Meissner, Phys. Rev. **140**, A1568 (1965).

[13]M. Tinkham, *Introduction to Superconductivity* (McGraw-Hill, New York, 1975).

[14]D. C. Mattis and J. Bardeen, Phys. Rev. **111**, 41 (1958).

[15]J. Gittleman and B. Rosenblum, Proc. IEEE 52, 1138 (1964).

[16]S. Skalski, O. Betbeder-Matibet, and P. R. Weiss, Phys. Rev. **136**, A1500 (1964); K. Maki, in *Superconductivity,* edited by R. D. Parks (Marcel Dekker, New York, 1969).

[17]A. Schmid, in Ref. 8, Chap. 14.

[18]V. L. Ginzburg and L. D. Landau, Zh. Eksp. Teor. Fiz. **20**, 1064 (1950).

[19]J. I. Gittleman, B. Rosenblum, T. E. Seidel, and A. W. Wicklund, Phys. Rev. **137**, A527 (1965).

[20]M. P. Garfunkel, Phys. Rev. **173**, 516 (1968).

[21]B. D. Josephson, J. Phys. F **4**, 751 (1974).

[22]P. L. Richards, Phys. Rev. **126**, 912 (1962).

[23]S. Sridhar and J. E. Mercereau, Phys. Lett. **75A**, 392 (1980).

[24]R. Peters and H. Meissner, Phys. Rev. Lett. **30**, 965 (1973).

[25]A. Schmid, Phys. Rev. **186**, 420 (1969).

[26]A. J. Ritger and Hans Meissner, J. Low Temp. Phys. **40**, 495 (1980).

[27]Yu N. Ovchinnikov, A. Schmid, and Gerd Schön, Phys. Rev. Lett. **46**, 1013 (1981).

[28]E. P. Raynes, Ph.D. thesis, Cambridge University, 1971.